Applied Energy 266 (2020) 114823

Contents lists available at ScienceDirect

Applied Energy

journal homepage: www.elsevier.com/locate/apenergy

Probabilistic solar power forecasting based on weather scenario generation

Mucun Sun, Cong Feng, Jie Zhang*

The University of Texas at Dallas, Richardson, TX 75080, USA

HIGHLIGHTS

- Develop a weather scenario generation-based probabilistic forecasting model.
- Use Copula to model correlation between weather variables.
- Gibbs sampling is adopted to improve the weather scenario generation efficiency.
- Different weather scenario generation models are compared.
- Improve pinball loss by up to 140% compared to benchmark models.

ARTICLE INFO

Keywords:
Probabilistic solar power forecasting
Weather scenario generation
Gibbs sampling
Gaussian mixture model
Copula

ABSTRACT

Probabilistic solar power forecasting plays an important role in solar power grid integration and power system operations. One of the most popular probabilistic solar forecasting methods is to feed simulated explanatory weather scenarios into a deterministic forecasting model. However, the correlation among different explanatory weather variables are seldom considered during the scenario generation process. This paper presents an improved probabilistic solar power forecasting framework based on correlated weather scenario generation. Copula is used to model a multivariate joint distribution between predicted weather variables and observed weather variables. Massive weather scenarios are obtained by deriving a conditional probability density function given a current weather prediction by using the Bayesian theory. The generated weather scenarios are used as input variables to a machine learning-based multi-model solar power forecasting model, where probabilistic solar power forecasts are obtained. The effectiveness of the proposed probabilistic solar power forecasting framework is validated by using seven solar farms from the 2000-bus synthetic grid system in Texas. Numerical results of case studies at the seven sites show that the developed probabilistic solar power forecasting methodology has improved the pinball loss metric score by up to 140% compared to benchmark models.

1. Introduction

Solar power is one of the most promising renewable energy sources in the world due to its sustainability. According to the U.S. solar market insight report, the U.S. has installed 67 GW of photovoltaic (PV) by Q1 2019, with an expectation of doubling the installed PV capacity by 2024 [1]. However, the uncertain and variable nature of PV power makes it challenging to be integrated into power systems, particularly at ever-increasing level of solar penetration. Therefore, accurate solar forecasting is needed to assist power system operation and planning, from day-ahead forecasts for unit commitment to minutes- and hours-ahead forecasts for economic dispatch.

A collection of deterministic solar power forecasting methods have been developed in the literature in the past years. Solar power forecasting methods can be generally classified into three groups [2]: (1) Physical models, which are usually developed based on the interaction between sophisticated meteorological variables and solar radiation. Physical solar forecasting models include sky imagery models [3], numerical weather prediction (NWP) models [4], and satellite imaging models [5]. Physical models usually require high computation cost, and have better performance than purely statistical time series approaches in longer prediction time horizons (e.g., day-ahead and week-ahead) [6]. (2) Statistical models, which extract information from historical data and quantify the relationship between solar power/irradiance and explanatory variables or lagged time series to generate forecasts. Statistical models are cost-saving since they do not require any expensive simulations beyond historical solar power generation after being trained. However, the prediction performance of statistical models drops with the increase of prediction time horizon [7]. (3) Hybrid or ensemble models, which combine two or more methods together

* Corresponding author.
E-mail address: jiezhang@utdallas.edu (J. Zhang).

https://doi.org/10.1016/j.apenergy.2020.114823
Received 24 December 2019; Received in revised form 26 February 2020; Accepted 8 March 2020
Available online 19 March 2020
0306-2619/

Nomenclature

Acronyms

PV	photovoltaic
KDE	kernel density estimation
GHI	global horizontal irradiance
WS	wind speed
TEMP	temperature
EM	expectation maximization
CDF	cumulative density function
NWP	numerical weather prediction
NRMSE	normalized root mean square error
NMAE	normalized mean absolute error
PS	persistence of cloudiness
QR	quantile regression
FD	fixed-date
SD	shifted-date
BS	bootstrap
PIs	prediction intervals
PDF	probability density function
GMM	Gaussian mixture model
wsp − WPF	weather scenario generation-based probabilistic forecasting
M3	machine learning-based multi-model
HA	hour ahead

Variables and Functions

$f_G(\cdot)$	probability density function of Gaussian mixture model
$g_i(\cdot)$	probability density function of the ith Gaussian mixture component
$F_G(\cdot)$	cumulative density function of Gaussian mixture model
$erf(\cdot)$	Gaussian error function
$C(\cdot)$	Copula function
$c(\cdot)$	Copula density function

Parameters

t	time index
$q_{m,t}$	mth quantile of solar power at time t
N_G	number of Gaussian mixture model components
$\vec{f}$	vector of weather forecasts
$\vec{a}$	vector of weather observation
$x_{f,j}$	forecast value of the jth weather variable
$x_{a,j}$	observation of the jth weather variable
$L_{m,t}$	pinball loss of the mth quantile at time t
p_t	solar power observation at time t

to obtain globally optimal forecasts. Hybrid methods have shown better predictive performance compared to single models [8].

PV power output is highly dependent on external weather conditions such as solar radiation and temperature [9]. Therefore, it is challenging to get accurate forecasts under different weather conditions. To better account for the solar power uncertainty and variability, probabilistic solar power forecasts are needed. Probabilistic solar power forecasts usually take the form of prediction intervals, quantiles, or predictive distributions. Generally, probabilistic solar power forecasting methods can be classified into parametric and nonparametric approaches [10]. Parametric approaches generally require low computational cost since a prior assumption of the predictive distribution shape is made before the parameter estimation. One of the most popular parametric methods is to convert point forecasts to probabilistic forecasts through a pre-defined predictive distribution. For example, Sun et al. [10] built a predictive distribution pool with four different predictive distributions, and the distribution with the minimum pinball loss was selected as the best predictive distribution. However, studies showed that unimodal distributions might not accurately quantify the variability of solar power due to the multi-modality nature in solar power predictive distributions [11,12]. Nonparametric approaches are distribution free, and their predictive distributions are inferred through observations or scenarios. To the best of authors' knowledge, most of probabilistic solar power forecasting papers in the literature focused on nonparametric methods. In a review study by Van der Meer et al. [13], the family of nonparametric approaches dominate methods of probabilistic solar power forecasting by accounting for 69% of all reviewed studies. These nonparametric probabilistic solar forecasting methods mainly include quantile regression-based methods [14,15], Gaussian process [16,17], simulating predictors [18,19], gradient boosting-based methods [20], and analog ensemble methods [21,22]. Among these aforementioned probabilistic solar power forecasting models, quantile regression-based methods and simulating predictors are more popular due to their simplicity. For quantile regression-based methods, parameters of different regression models could be optimized through minimizing a loss function. Therefore, different regression models could be integrated with probabilistic forecasting metrics such as pinball loss, continuous ranked probability score, and brier score. For example, Wang et al. [23] formulated quantile regression as an optimization problem to minimize the pinball loss. Three regression models, namely, neural network, random forests, and gradient boosting, were integrated with quantile regression to generate probabilistic forecasts.

For methods with simulating predictors, massive scenarios are generated as inputs of regression models. Weather scenario generation has been widely used in the literature for probabilistic forecasts due to its simplicity and accessibility. Weather scenario generation methods can be generally classified into three categories [24]: (i) fixed-date method, (ii) shifted-date method, and (iii) bootstrap method. The fixed-date method assigns the weather profile of historical years to the current year. The number of scenarios equals to the number of years the weather profile is available. For example, Liu et al. [25] used six years historical weather data as input scenarios to a quantile regression averaging model. The shifted-date method generally shifts the historical weather profile with a number of days. Then these shifted weather profiles are treated as weather scenarios of the current year. The number of scenarios generated by the fixed-date and shifted-date methods is limited by the length of the weather profile and data availability. Bootstrap is a method of computational inference based on resampling a dataset. Breinl et al. [26] adopted a block bootstrap method to generate precipitation and temperatures scenarios. However, scenarios generated from block bootstrap heavily relied on the data itself and block size, where extreme weather observations tend to be undervalued. The three weather scenario generation methods mentioned above were compared in [24] through quantile score, complexity, and number of scenarios based on the GEFCom2014 dataset. Results showed that among the bootstrap, fixed-date, and shifted-date methods, no single method outperforms others in all aspects. In addition, a study has shown that the exogenous atmospheric variables used in solar power forecasting are spatial-temporal correlated [27]. However, all the aforementioned weather scenario generation methods didn't take the correlations among weather variables into account. Ignoring the correlation characteristics in weather scenario generation modeling may lead to inaccurate results in simulated predictors, which may further affect the probabilistic forecasting accuracy.

One of the most intuitive ways of modeling correlation among different variables is to use a multivariate joint distribution. To address the challenge of modeling high dimensional multivariate joint distributions, the Copula theory can be used. Based on the Sklar's theorem, the joint distribution can be modeled through univariate marginal distributions and a Copula [28]. In [29], a Copula method was adopted to model the dependencies between solar power and ambient temperature. However, high dimensional matrices are involved in sampling from the conditional distributions, which is not

computationally efficient.

To address the aforementioned challenges, in this paper, we seek to develop a probabilistic solar power forecasting method based on weather scenario generation considering inherent correlation among different weather variables. The principle of this method is the use of a multivariate joint probability density function (PDF) of historical actual weather variables and historical predicted weather variables. The conditional distribution of historical actual weather given historical weather forecasts is deduced through the Bayesian theory, which is then used (in conjunction with current weather deterministic forecasts) to generate massive weather scenarios through an efficient Gibbs sampling model. By feeding these weather scenarios as inputs into a pre-trained deterministic solar forecasting model, we can generate a same number of solar power scenarios at each time step. Probabilistic forecasts are finally generated in the form of quantiles through the empirical distribution of solar power scenarios. Main contributions of this paper are summarized as follows:

1. An improved probabilistic solar power forecasting method is developed based on weather scenario generation;
2. Copula is used to model the correlation among weather variables to improve the performance of weather scenario generation;
3. A Gaussian mixture model is used to accurately fit the marginal distributions of different weather variables;

The rest of the paper is organized as follows. Section 2 describes the proposed weather scenario generation-based probabilistic solar power forecasting method, which consists of a deterministic forecasting method, Gaussian mixture model-based marginal weather probability distribution modeling, and a Copula-based Gibbs sampling model. Section 3 applies the developed probabilistic solar forecasting method to 7 solar farms and compares the proposed method with four benchmark probabilistic solar power forecasting models. Concluding remarks and future work are discussed in Section 4.

2. Probabilistic forecasting framework

The overall framework of the developed weather scenario generation-based probabilistic solar power forecasting (wsp-SPF) method is illustrated in Fig. 1. The two major steps are weather scenario generation and probabilistic solar power forecasting. In each major step, there are several sub-steps which are briefly described as follows:

1. Step 1.1: A Machine Learning-based Multi-Model (M3) forecasting framework is adopted to generate short-term deterministic weather forecasts (i.e., 1-h-ahead (1HA)), and train the deterministic solar power forecasting model (blue box).
2. Step 1.2: A Gaussian mixture model (GMM) is used to fit the PDFs of historical actual weather and historical forecasted weather.
3. Step 1.3: The conditional joint distribution of historical actual weather given historical weather forecasts is constructed based on the Copula theory.
4. Step 1.4: A large number of weather scenarios are generated through the conditional distribution via Gibbs sampling.
5. Step 2: The simulated weather predictors are fed into the pre-trained M3 deterministic solar power forecasting model to generate probabilistic solar power forecasts.

2.1. Machine learning-based multi-model (M3) deterministic forecasting

In this paper, the M3 model developed in our previous work [6] is adopted to train deterministic forecasting models (i.e., deterministic weather forecasting model and deterministic solar power forecasting model). M3 is ensembled by multiple models from a pool of state-of-the-art machine learning-based forecasting models. To be more specific, multiple sets of deterministic forecasts are generated by using different machine learning algorithms with different kernels in the first layer. Then, the forecasts are blended by another machine learning algorithm in the second layer to generate final forecasts. Machine learning algorithms used in the M3 method include artificial neural networks

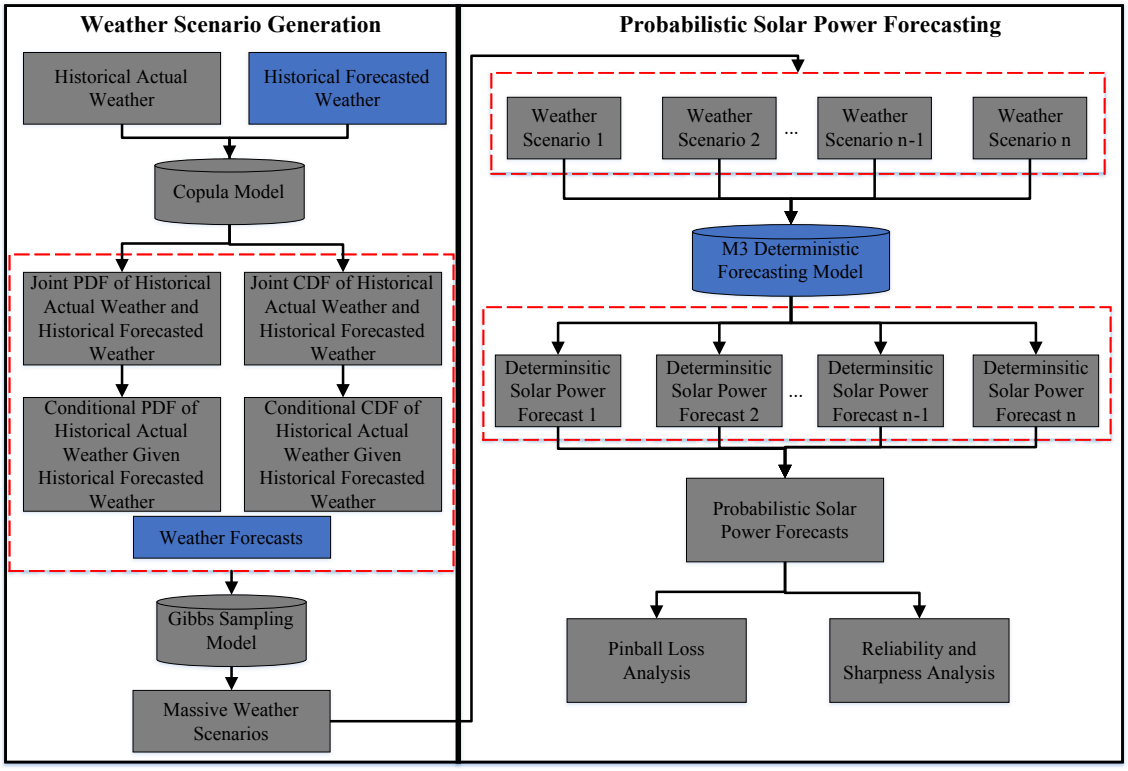

Fig. 1. Overall framework of weather scenario generation-based probabilistic solar power forecasting.

(ANNs), support vector regression (SVR), gradient boosting machines (GBMs), and random forests.

2.2. Weather distribution modeling

In the literature, marginal distributions of weather variables are commonly modeled by unimodal distributions such as Beta and Gamma [30] or nonparametric distributions such as kernel density estimation (KDE) [31]. However, unimodal distributions may not accurately quantify the variability of weather variables and nonparametric distributions are challenging to be solved analytically [32]. Mixture distributions have been widely utilized in statistics to approximate multimodal distributions. To accurately characterize the variability of weather variables, GMM is adopted in this paper to model the weather variables. Three weather variables are considered in this paper, which are global horizontal irradiance (GHI), wind speed (WS), and temperature (TEMP). The PDF of GMM is formulated as follows:

$$f_G\left(x\middle|N_G, \omega_i, \mu_i, \sigma_i\right) = \sum_{i=1}^{N_G} \omega_i g_i\left(x\middle|\mu_i, \sigma_i\right) \tag{1}$$

where N_G is the number of mixture components, $U(\mu_i \in U)$ is an expected value vector, $\Sigma(\sigma_i \in \Sigma)$ is a standard deviation vector, and $\Omega(\omega_i \in \Omega)$ is a weight vector. Each component $g(x;\mu_i, \sigma_i)$ follows a normal distribution, which is expressed as:

$$g_i\left(x\middle|\mu_i, \sigma_i\right) = \frac{1}{\sqrt{2\pi\sigma_i^2}} e^{-\frac{(x-\mu_i)^2}{2\sigma_i^2}} \tag{2}$$

The GMM distribution has two constraints: (1) the integral of Eq. (1) equals unity, and (2) the summation of weight parameters equals unity as well, which are expressed as follows:

$$\int_{-\infty}^{+\infty} f_G\left(x\middle|N_G, \omega_i, \mu_i, \sigma_i\right)dx = \int_{-\infty}^{+\infty} \sum_{i=1}^{N_G} \omega_i g_i\left(x\middle|\mu_i, \sigma_i\right)dx = 1 \tag{3}$$

$$\sum_{i=1}^{N_G} \omega_i = 1 \tag{4}$$

The parameters of GMM are estimated by the expectation maximization (EM) algorithm. The goal of EM is to maximize the likelihood function with respect to parameters. More details about EM can be found in [33]. The cumulative density function (CDF) (F_G) corresponding to the estimated PDF is expressed as:

$$F_G\left(x\middle|N_G, \omega_i, \mu_i, \sigma_i\right) = \sum_{i=1}^{N_G} \left[\frac{\sqrt{\pi}}{2}\omega_i\sigma_i erf\left(\frac{\mu_i - x}{\sigma_i}\right)\right] + C \tag{5}$$

where C is an integral constant, and $erf(\cdot)$ is a Gaussian error function.

2.3. Weather scenario generation

Once marginal distributions of historical actual and predicted weather variables are defined, the correlation among weather variables can be modeled through a multivariate joint distribution. The parameter $x_{f,j}$ denotes the forecast value of the jth weather variable, and $x_{a,j}$ denotes the actual value of the jth weather variable. We assume there are J weather variables. The parameter $\vec{f}$ denotes the J-dimension vector of weather forecasts, i.e., $(x_{f,1}, ...,x_{f,J})$; $\vec{a}$ denotes the J-dimension vector of actual weather, i.e., $(x_{a,1}, ...,x_{a,J})$. The joint CDF and joint PDF are expressed as:

$$F(a, f) = P(X_{a,1} \leqslant x_{a,1}, ...,X_{a,J} \leqslant x_{a,J}, X_{f,1} \leqslant x_{f,1}, ...,X_{f,J} \leqslant x_{f,J}) \tag{6}$$

$$f\left(a, f\right) = \frac{\partial^{2J}F(a, f)}{\partial X_{a,1}...\partial X_{a,J}\partial X_{f,1}...\partial X_{f,J}} \tag{7}$$

Therefore, the weather scenario generation given predicted weather becomes sampling a multivariate distribution of the actual weather a, i.e., $(x_{a,1}, ...,x_{a,J})$, conditioning on the predicted weather f, i.e., $(x_{f,1}, ...,x_{f,J})$.

$$F(a|f) = P(X_{a,1} \leqslant x_{a,1}, ...,X_{a,J} \leqslant x_{a,J}|X_{f,1} = x_{f,1}, ...,X_{f,J} = x_{f,J}) \tag{8}$$

$$f\left(a\middle|f\right) = \frac{\partial^{J}F(a|f)}{\partial X_{a,1}...\partial X_{a,J}} \tag{9}$$

In this study, Copula is used to model the inherent correlation among weather variables, and the conditional multivariate distribution is modeled based on the aforementioned weather marginal distributions. Given a multivariate joint distribution, it is challenging to directly generate samples due to the high dimensionality of conditioning variables. In this paper, Gibbs sampling is applied to sample the multidimensional random variables by sequentially sampling each component.

2.3.1. Gibbs sampling

Gibbs sampling seeks to iteratively sample only one variable or a block of variables at a time from its distribution conditioned on the remaining variables [34]. Therefore, Gibbs sampling converts sampling a multivariate distribution into sampling a set of conditional univariate distributions. The pseudocode of Gibbs sampling is illustrated in Algorithm 1. Note in this study, we use the forecasted weather as the initial input.

Algorithm 1. Gibbs sampling

Result: Weather scenarios

initialization: $x_{a,j}^0 \leftarrow x_{f,1}, \forall j = 1, ..., J$;

for *scenario* $\eta = 1, ...,$ **do**

  $X_{a,1}|x_{a,2}^{(\eta-1)}, ..., x_{a,J}^{(\eta-1)}$;

  $X_{a,2}|x_{a,1}^{(\eta)}, x_{a,3}^{(\eta-1)}, ..., x_{a,J}^{(\eta-1)}, x_{f,1}, ..., x_{f,J}$;

  ...

  $X_{a,J}|x_{a,1}^{(\eta)}, ..., x_{a,J-1}^{(\eta)}, x_{f,1}, ..., x_{f,J}$

end

Table 1
Data summary of the selected 7 solar sites

Site Name	Site ID	Lat.	Long.	Capacity (MW)	State
C1	3	29.58	−104.29	10	TX
C2	21	32.26	−101.41	1.5	TX
C3	22	32.25	−101.42	230	TX
C4	109	29.32	−100.38	29.7	TX
C5	286	30.55	−97.69	1.05	TX
C6	287	30.55	−97.69	22.5	TX
C7	288	30.54	−97.69	5.5	TX

2.3.2. Conditional distribution modeling

Copula is one of the most widely used methods for modeling the dependency among random variables. Based on Sklar's theorem [35], any multivariate joint distribution can be written in terms of univariate marginal distribution functions and a copula that describes the dependence structure between the variables. Therefore, the joint CDF in Eq. 6 can be written as:

$$F(a, f) = C(F(x_{a,1}), \ldots, F(x_{a,J}), F(x_{f,1}), \ldots, F(x_{f,J})) = C(S, T) \tag{10}$$

where,

$$S = F(x_{a,1}), \ldots, F(x_{a,J}) \tag{11}$$

$$T = F(x_{f,1}), \ldots, F(x_{f,J}) \tag{12}$$

$F(x_{a,j})$ and $F(x_{f,j})$ denote the marginal CDFs of actual weather and marginal CDF of predicted weather, respectively. $C(\cdot)$ is the Copula function.

Similarly, the joint PDF of actual weather and predicted weather can be expressed as:

$$f\left(a, f\right) = c\left(S, T\right) \cdot \prod_{j=1}^{J} \left(f(x_{a,j}) f(x_{f,j})\right) \tag{13}$$

where $f(x_{a,j})$ and $f(x_{f,j})$ are marginal PDFs of $X_{a,j}$ and $X_{f,j}$, respectively, modeled by using the aforementioned GMM distribution based on historical actual and forecasting weather. $c(\cdot)$ is the density of Copula. Then, the conditional univariate distribution of weather variable $X_{a,j}$ can be deduced from the Bayesian formula, given by:

$$\begin{aligned} &F(x_{a,j} | x_{a,1}, \ldots, \quad x_{a,j-1}, x_{a,j+1}, \ldots, x_{a,J}, f) \\ &= \quad \frac{P(X_{a,j} \leqslant x_{a,j}, X_{a,p} = x_{a,p}, X_{f,q} = x_{f,q})}{P(X_{a,p} = x_{a,p}, X_{f,q} = x_{f,q})} \\ &\qquad p = 1, \ldots, j-1, j+1, \ldots, J, \qquad q = 1, \ldots, J \end{aligned} \tag{14}$$

where the numerator can be written as:

$$\begin{aligned} P\left(X_{a,j} \leqslant x_{a,j}, X_{a,p} = x_{a,p}, X_{f,q} = x_{f,q}\right) &= \int_0^{x_{a,j}} f\left(a, f\right) dX_{a,j} \\ &= \int_0^{x_{a,j}} c(\cdot) \prod_{p=1}^{J} f(x_{a,p}) f(x_{f,p}) dX_{a,j} \end{aligned} \tag{15}$$

and based on Eq. (13), the denominator can be written as:

$$P\left(X_{a,p} = x_{a,p}, X_{f,q} = x_{f,q}\right) = c'(\cdot) \frac{\prod_{p=1}^{J} \left(f(x_{a,p}) f(x_{f,p})\right)}{f(x_{a,j})} \tag{16}$$

Note that in Eq. (16), we use $c'(\cdot)$ instead of $c(\cdot)$ since the dimension of Copula density here is $2J-1$ instead of $2J$. Overall, based on Eqs. (15) and (16), the conditional univariate CDF can be expressed as:

$$\begin{aligned} &F\left(x_{a,j} \middle| x_{a,1}, \ldots, x_{a,j-1}, x_{a,j+1}, \ldots, x_{a,J}, f\right) \\ &= \frac{\partial^{2J-1} C(\cdot)}{\partial X_{a,1} \ldots \partial X_{a,j-1} \partial X_{a,j+1} \ldots \partial X_{a,J} \partial X_{f,1} \ldots \partial X_{f,J}} \cdot \frac{1}{c'(\cdot)} \end{aligned} \tag{17}$$

The conditional distribution of the actual weather variable given weather forecasts can be trained by using historical actual and forecasted weather data. With any given deterministic weather forecasts, the Gibbs sampling model and the trained conditional CDF in Eq. (17) are used together to generate a large number of weather scenarios. In this study, the Copula is selected through the "xvCopula" function from the **Copula** package [36] in R based on k-fold cross-validation.

2.4. Probabilistic solar power forecasting

Once weather scenarios are given, a large number of solar power scenarios can be generated through a deterministic forecasting model. Assuming that we generate N weather scenarios for each hour, then we will have N deterministic solar power forecast values for each hour. Therefore, based on the empirical distribution function, the 1st to 99th percentiles of solar power can be calculated for each hour, thus generating probabilistic solar power forecasts. Though any deterministic forecasting model is capable of generating solar power forecasts, we adopted the M3 model mentioned in Section 2.1.

3. Case studies and results

This section describes the dataset used in the paper and analyzes the probabilistic solar power forecasting results based on weather scenario generation. The objectives of this study are: (1) develop an improved probabilistic solar power forecasting method based on weather scenario generation considering correlation among different weather variables; (2) compare different state-of-the-art weather scenario generation methods; (3) integrate Gibbs sampling to the scenario generation process to improve computational efficiency.

3.1. Data summary

The developed wsp-SPF framework is evaluated at 7 solar farms in Texas that are selected from the ACTIVSg2000 system, i.e., a 2000-bus synthetic grid on the footprint of Texas [37]. The data information at the 7 selected solar sites is briefly summarized in Table 1. To ensure the generality and diversity of data, some of the selected solar farms are closed to each other (e.g., C2 and C3; C5, C6, and C7), and some of the solar farms are geographically dispersed (e.g., C1 and C4). In addition, all the selected solar farms have different capacity which ranges from 1.05 MW to 230 MW. To match the solar power with corresponding weather information, the weather data is collected from the National Solar Radiation Database (NSRDB) [38]. The NSRDB includes solar radiation and other meteorological information (e.g., wind speed, air temperature, solar zenith angle) over the United States from 1998 to 2017 computed by the National Renewable Energy Laboratory's (NREL's) Physical Solar Model (PSM), with a 30 min temporal resolution. The solar power is generated based on NSRDB weather data using System Advisor Model (SAM) [39], and shares the same resolution with weather data. In this study, the duration of the collected data at the 7 selected solar sites spans four years from January 1st 2008 to December 31st 2011. Fig. 2 summaries the data partition of the case study. For all the 7 locations, the first 3/4 of the data is used as training data, in which the first 2/3 is used to train the deterministic weather forecasting model and the remaining 1/3 of the training data is used to train the conditional weather scenario model. The accuracy of the forecasts is evaluated by the remaining 1/4 of data. The number of weather scenarios generated from the conditional distribution is set as $N_s = 5{,}000$. Though the developed wsp-SPF method is capable of generating

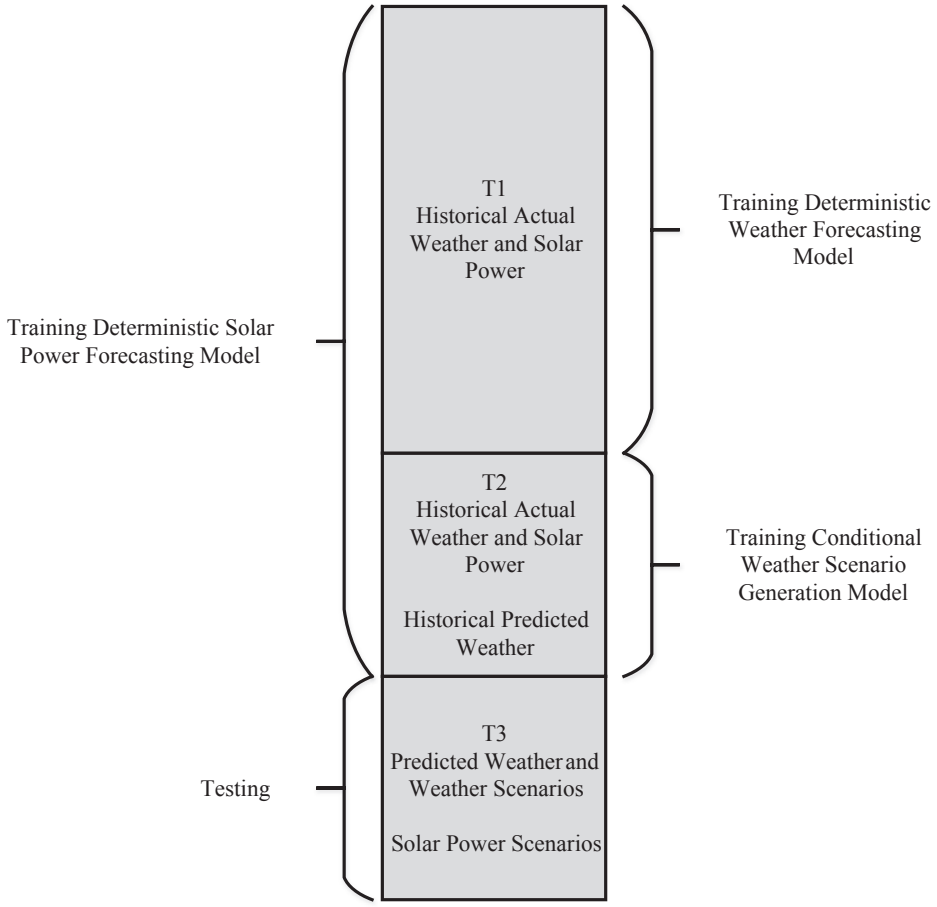

Fig. 2. Data splitting for model training and testing.

forecasts at multiple forecasting horizons, only 1-h-ahead solar power forecasts are explored in this study.

3.2. Deterministic forecasting results

Since the Copula-based weather scenario generation method is a two-step method, it is important to compare the performance of different deterministic forecasting models in the first step. Normalized indices of standard metrics like root mean squared error and mean absolute error, *i.e.*, NRMSE and NMAE, are adopted to evaluate the performance of deterministic forecasts. They are defined by:

$$NMAE = \frac{1}{T}\sum_{t=1}^{T}\left|\frac{\hat{x}_t - x_t}{x_{max}}\right| \times 100\% \tag{18}$$

$$NRMSE = \frac{1}{x_{max}}\sqrt{\frac{\sum_{t=1}^{T}(\hat{x}_t - x_t)^2}{T}} \times 100\% \tag{19}$$

where $\hat{x}_t$ is the forecasted weather variable, x_t is the observation of the weather variable, x_{max} is the maximum observation of the corresponding weather variable, and T is the sample size.

A smaller NRMSE or NMAE indicates better forecasting performance. The 1HA deterministic forecasting errors by using the M3

Table 2
1HA deterministic weather forecasting results by using M3 and PS.

Model	Feature	Metric	Site						
			C1	C2	C3	C4	C5	C6	C7
M3	GHI	NMAE(%)	4.32	3.98	4.11	4.23	3.53	3.72	3.48
		NRMSE(%)	7.16	6.59	6.81	6.99	5.91	6.21	5.94
	WS	NMAE(%)	1.82	1.96	1.89	1.83	1.77	1.77	1.81
		NRMSE(%)	2.74	2.92	2.77	2.60	2.47	2.49	2.53
	TEMP	NMAE(%)	1.91	1.68	1.69	1.69	1.35	1.36	1.36
		NRMSE(%)	2.46	2.19	2.19	2.15	1.79	1.79	1.79
PS	GHI	NMAE(%)	6.79	6.63	6.63	6.62	6.59	6.60	6.57
		NRMSE(%)	10.84	10.79	10.79	10.95	11.00	11.01	10.94
	WS	NMAE(%)	3.10	3.61	3.61	3.34	3.31	3.31	3.31
		NRMSE(%)	4.60	5.27	5.27	4.85	4.91	4.91	4.91
	TEMP	NMAE(%)	2.57	2.23	2.23	2.31	2.12	2.12	2.11
		NRMSE(%)	3.40	3.07	3.07	3.13	2.94	2.94	2.94

deterministic forecasting model at the selected locations are summarized in Table 2. The persistence of cloudiness method (PS) [40] has been proved to be accurate in the shorter forecasting period. Therefore, to show the superiority of the M3 deterministic forecasting model, the PS method is adopted as the baseline. Overall, the accuracies of the M3 deterministic forecasts are better than those of persistence of cloudiness forecasts.

3.3. Benchmarks and comparison settings

In this paper, four benchmark models are selected for comparison, including one single probabilistic forecasting baseline model, and three other weather scenario generation-based models. The single benchmark model is quantile regression (QR). The three benchmark weather scenario generation models are fixed-date (FD), shifted-date (SD), and bootstrap (BS) methods, which have been used by Xie et al. in [24]. Note that the same M3 deterministic forecasting model is used in the three weather scenario generation-based models.

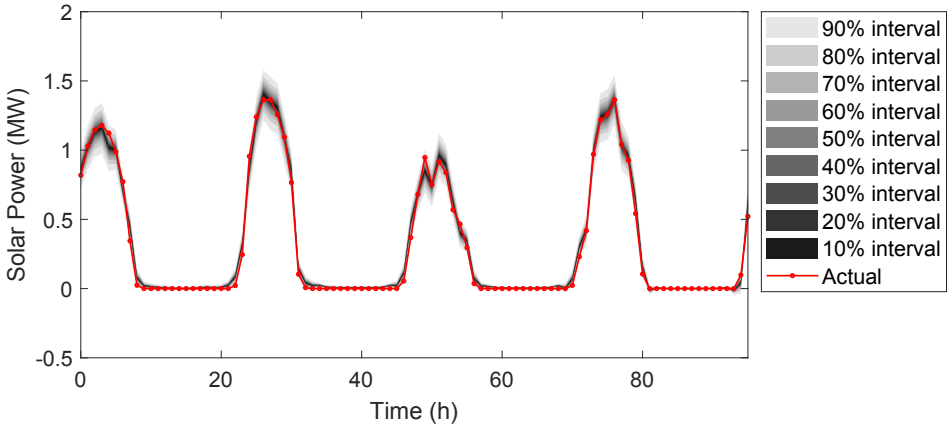

(a) wsp-SPF

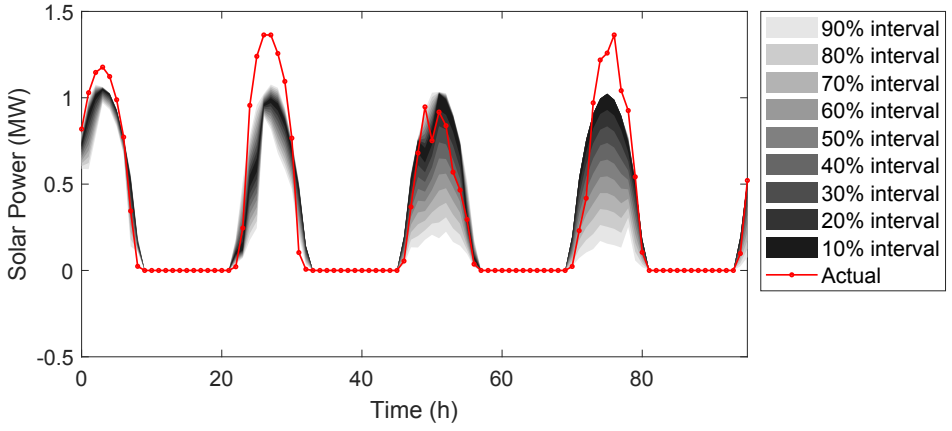

(b) M3-FD

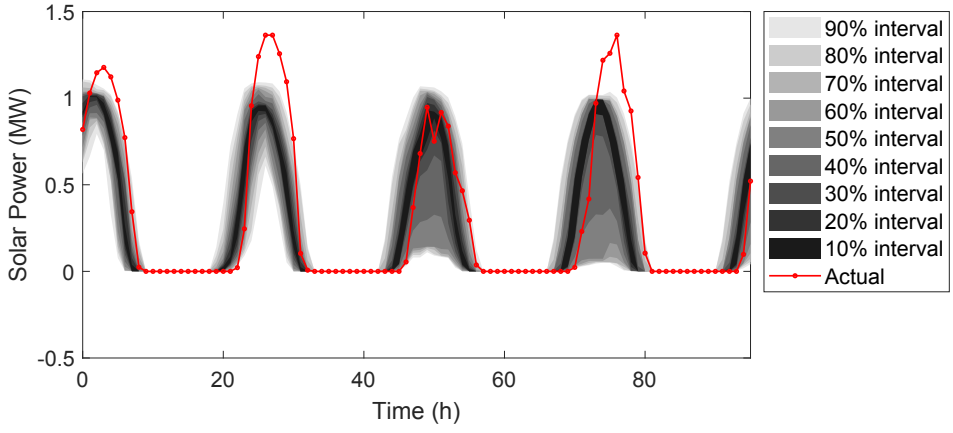

(c) M3-SD

Fig. 3. 1HA probabilistic solar power forecasts.

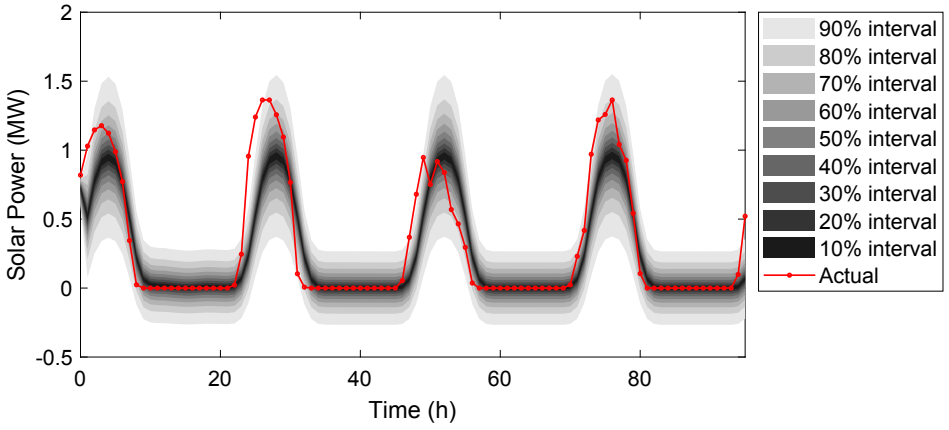

(d) M3-BS

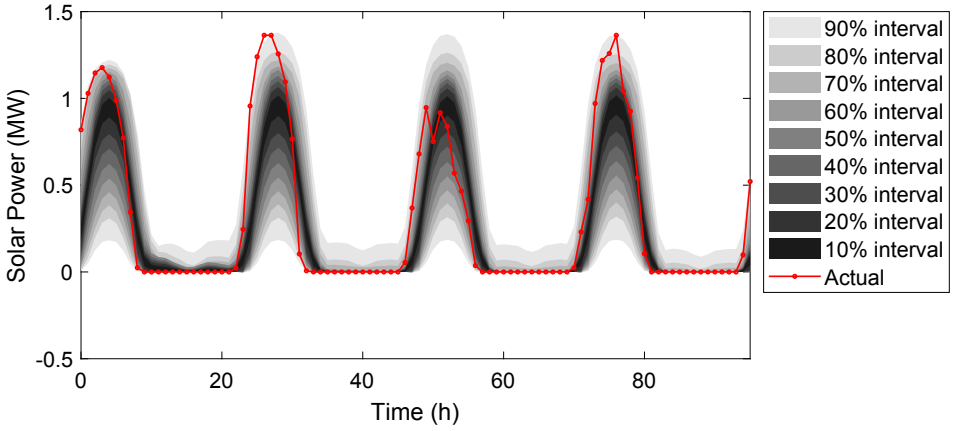

(e) QR

Fig. 3. (*continued*)

1. FD: The fixed-date method assigns the weather profile of historical years to the current year. The number of scenarios equals to the number of years the weather profiles is available. Assume that m years weather profiles are available, we could generate m weather scenarios at each time step.
2. SD: The shifted-date method generally shifts the historical weather profile with a number of days. Then these shifted weather profiles are treated as weather scenarios of the current year. Assume that m years weather profiles are available, we could generate $(2n + 1)m$ weather scenarios at each time step, where n is the number of days shifted forward or backward. The n is set to be 4 in this study.
3. BS: The bootstrap method divides the weather profile of each historical year into an equal length of blocks, and then randomly picks the blocks with replacement from any of the historical years to form a new temperature profile. In this study, we set the block length be 10. Overall, there are 37 blocks, where each of the first 36 blocks has a length of 10 and the $37th$ block has a length of 5.

The reasons for choosing these four baseline models are: (i) QR is a widely used method in probabilistic forecasting, which allows us to explore the forecasting enhancement by considering weather scenario generation; (ii) since a weather scenario generation model is included in the proposed wsp-SPF method, it is important to compare the accuracy of the proposed method with different weather scenario generation techniques. Note that the empirical probability distribution is adopted to calculate the quantile forecasts. However, for the FD and SD methods, the number of both weather and solar power scenarios is limited. As a result, some of the adjacent quantiles may share a same value.

3.4. Probabilistic forecasting results

Once solar power scenarios are generated, quantiles of the solar power are calculated based on the empirical distribution of the generated scenarios.

With the estimated empirical predictive PDF of the solar power, the quantiles q_1, q_2, …, q_{99} can be calculated. To better visualize probabilistic forecasts, the 99 quantiles are converted into nine prediction intervals (PIs) I_β ($\beta = 10$, …, 90) in a 10% increment. Fig. 3(a) shows the 1HA probabilistic solar power forecasts of the C2 site from 2011-01-31 to 2011-02-03, generated from the proposed wsp-SPF model. It is

Table 3
Normalized pinball loss and relative improvement of different models.

	Model	Site						
		C1	C2	C3	C4	C5	C6	C7
NPL	wsp-SPF	**1.77**	**1.62**	**1.75**	**2.13**	**1.35**	**1.49**	**1.46**
	M3-FD	1.86	2.07	2.08	2.43	2.38	2.38	2.34
	M3-SD	3.08	3.11	3.11	2.99	3.12	3.11	3.11
	M3-BS	3.09	3.43	3.74	2.94	3.74	3.27	3.29
	QR	2.46	2.64	2.64	2.44	1.40	2.66	2.64
IP (%)	M3-FD	5.08	27.78	18.86	14.08	75.00	59.73	60.27
	M3-SD	74.01	91.97	77.71	*40.37*	128.68	108.72	113.01
	M3-BS	*74.58*	*111.72*	*113.71*	38.02	*140.44*	*119.46*	*125.34*
	QR	38.98	62.96	50.86	14.55	95.59	78.52	80.82

Note: The smallest normalized pinball loss value is in boldface. The highest relative improvement with respect to wsp-SPF model is in italic.

observed that at the entire representative period, the solar power reasonably lies within the PIs. Fig. 3(b), (c), (d) and (e) show the probabilistic forecasts generated from the baseline M3-FD, M3-SD, M3-BS, and QR methods, respectively. It is seen that the PIs of the wsp-SPF model in Fig. 3(a) is narrower than the PIs with other weather scenario generation methods. This is due to that considering the correlation among weather variables has improved the weather scenario generation accuracy. In addition, the PIs of wsp-SPF are smoother than those of QR, which indicates stable and reliable probabilistic forecasts. Among the three weather scenario generation-based baseline methods, M3-BS outperforms M3-FD and M3-SD. It is mainly due to the limited number of scenarios in FD and SD models. It is also observed that the width of the PIs varies with the variability of solar power. For example, when the solar power fluctuates more frequently, the PI tends to be wider, and thereby the uncertainty in solar power forecasts is relatively higher.

3.4.1. Pinball loss

Pinball loss is a widely used metric to evaluate the overall performance of probabilistic forecasts, which is defined by:

$$L_{m,t}\left(q_{m,t}, p_t\right) = \begin{cases} (1 - \frac{m}{100}) \times (q_{m,t} - p_t), & p_t < q_{m,t} \\ \frac{m}{100} \times (p_t - q_{m,t}), & p_t \geqslant q_{m,t} \end{cases} \tag{20}$$

where $q_{m,t}$ represents the mth quantile at time t, p_t represents the solar power observation at time t. To show the effectiveness of the developed weather scenario generation-based probabilistic forecasting framework, the normalized pinball loss (NPL) values of 1HA solar power forecasts from different models and their relative improvement (IP) with respect to wsp-SPF model are compared in Table 3. The sum of pinball loss is averaged over all quantiles from 1% to 99% and normalized by the solar power capacity. A lower pinball loss score indicates a better probabilistic forecast. Results show that the proposed wsp-SPF model gives the best performance. Moreover, the proposed wsp-SPF model has improved the pinball loss by 5.08%-140.44% compared to the four benchmark models, which validates the effectiveness of the proposed method. It is interesting to see the highest NPL improvement is from C5, which has the smallest solar capacity. This may be due to that solar farms with smaller capacity are more susceptible to weather conditions, thus the correlation between weather scenarios and PV power outputs becomes stronger. In contrast, for the solar farm with the largest

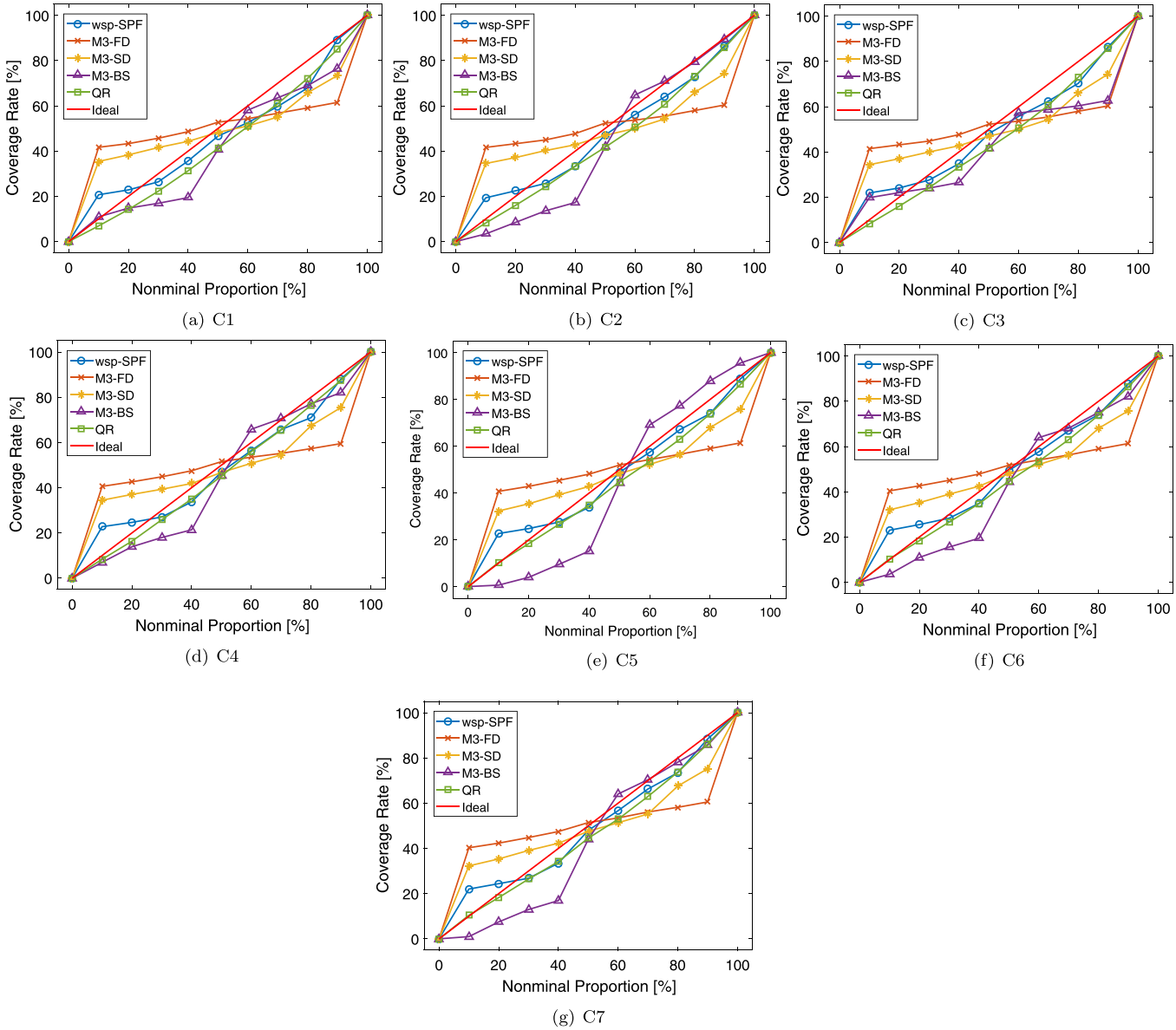

Fig. 4. Reliability comparison of different models at different sites.

capacity like C3, the NPL improvement is intermediate. Therefore, there is no clear linear relationship between the NPL improvement brought from weather scenario generation and the solar farm capacity. The improvement may result from different factors such as geographic location and capacity. Note that the wsp-SPF method has shown a better accuracy than M3-FD, M3-SD, and M3-BS, which indicates the

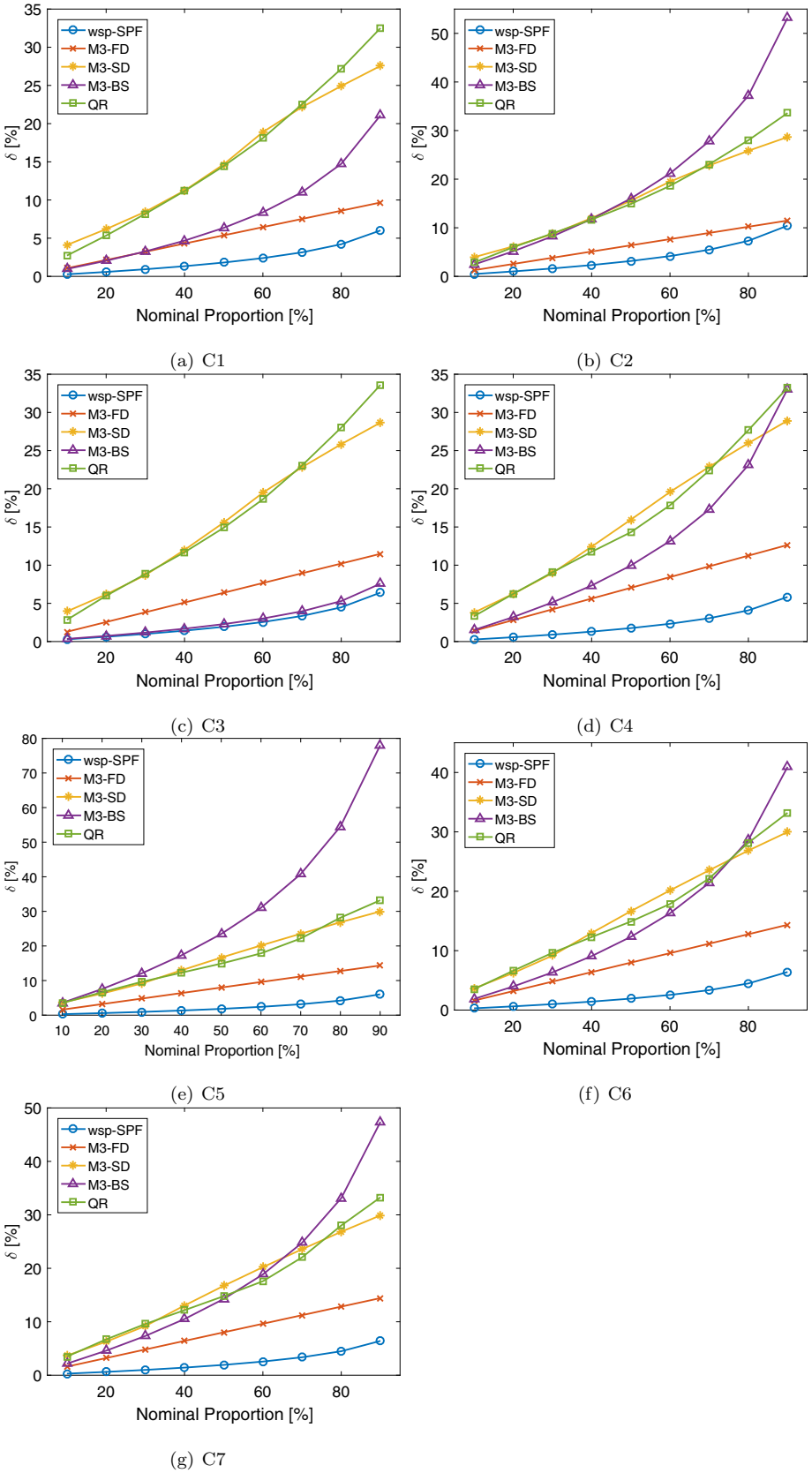

Fig. 5. Sharpness comparison of different models at different sites.

improvement of the weather scenario generation by considering the correlation among weather variables. Furthermore, the wsp-SPF model outperforms QR, which shows the improvement by considering weather scenario generation modeling. In addition to pinball loss, two more standard metrics, i.e., reliability and sharpness, are also calculated to assess the performance of wsp-SPF.

3.4.2. Reliability

Reliability (RE) stands for the correctness of a probabilistic forecast that matches the observation frequencies [10]:

$$RE = \left[\frac{\xi^{(1-\alpha)}}{N} - \left(1-\alpha\right)\right] \times 100\% \tag{21}$$

where N is the number of test samples, and $\xi^{(1-\alpha)}$ is the number of times that the actual test samples lie within the αth prediction interval. A reliability plot shows whether a given method tends to systematically underestimate or overestimate the uncertainty. In this study, the nominal coverage rate ranges from 10% to 90% with a 10% increment. Fig. 4 shows the reliability plots of the probabilistic solar power forecasts with different forecasting models at the 7 sites. A forecast presents better reliability when the curve is closer to the diagonal. It is seen from Fig. 4 that overall the proposed wsp-SPF has better reliability performance than M3-FD, M3-SD, and M3-BS, indicating the enhancement resulted from correlation modeling between weather variables. In addition, the proposed wsp-SPF model has shown similar reliability to QR, while the PIs of wsp-SPF are narrower than those of QR, which secure accuracy without sacrificing reliability. In addition, note that the reliability at C5 is worse than that at other solar farms, and C3 has the best reliability. It is mainly because C5 has the smallest capacity, which is susceptible to weather variation. In contrast, C3 has the largest capacity, which might be more reliable and stable.

3.4.3. Sharpness

Sharpness indicates the capacity of a forecasting system to forecast extreme probabilities [28]. This criterion evaluates the predictions independently of the observations, which gives an indication of the level of usefulness of the predictions. For example, a system that provides only uniformly distributed predictions is less useful for decision-making under uncertainty. Predictions with perfect sharpness are discrete predictions with a probability of one (i.e., deterministic predictions). The sharpness is measured by the average size of the prediction intervals. The sharpness plots of wsp-SPF and four baseline models at different sites are compared in Fig. 5. The expected interval size increases with increasing the nominal coverage rate, and the sharpness of the proposed wsp-SPF model is significantly better than that of the four baseline models. Overall, the interval size of the proposed cp-AWPF model ranges from 1% to 10%, which indicates low sharpness. In addition, wsp-SPF has significantly better sharpness than M3-FD, M3-SD, and M3-BS at all sites, which validates the enhancement of correlation modeling in weather scenario generation. Since all the sites share low sharpness, it is hard to conclude the relationship between site capacity and sharpness. Moreover, it is seen that for solar farms in the same region (similar longitude and latitude), the sharpness is also similar. This characteristic may be used for solar resource assessment.

4. Conclusion

In this paper, a weather scenario generation-based probabilistic solar power forecasting framework was developed. Gaussian mixture model was used to accurately model the weather marginal distributions. Copula was adopted to model the correlation among different weather variables through a high-dimensional joint distribution. Gibbs sampling was applied on the conditional CDF of the joint distribution to generate a large number of weather scenarios. Then, these weather scenarios are fed into a machine learning-based multi-model deterministic forecasting model to generate probabilistic solar power forecasts. Results at 7 selected solar farms showed that:

1. wsp-SPF could reduce the pinball loss score by up to 140% compared to four benchmark models.
2. The GMM model has shown better goodness-of-fit to weather distribution than single-distribution models and KDE.
3. Considering correlation among weather variables could enhance weather scenario generation, thus providing better probabilistic forecasting accuracy.
4. The developed wsp-SPF framework is robust for solar farms at different locations with different capacities.
5. wsp-SPF has shown better sharpness than models without using weather scenario generation and models with other weather scenario generation methods (i.e., FD, SD, and BS). The reliability of wsp-SPF is close to the ideal diagonal, which indicates reasonable reliability.

In summary, the use of probabilistic solar forecasts is still at its early stage. Probabilistic forecasts are only used in a primitive way in most systems, and there is not a systematic way to integrate them into system operation and scheduling routines. However, operators start to realize the importance of probabilistic forecasts in shaping more cost-effective, stable, and reliable power systems. The proposed wsp-SPF framework could be applied in the decision-making process of real-time unit commitment and economic dispatch and to inform the system operator of excessive ramp rates. In addition, this proposed wsp-SPF framework can also be used to promote the integration of probabilistic solar power forecasts in power systems by determining the requirements of ancillary services, such as non-spinning reserves and ramping reserves. Potential future work will (i) utilize the probabilistic solar power forecasting model in stochastic power system operations, and (ii) explore the influence of spatio-temporal correlations on weather scenario generation.

Declaration of Competing Interest

None.

Acknowledgement

This work was supported by the National Renewable Energy Laboratory under Subcontract No. XAT-8-82151-01 (under the U.S. Department of Energy Prime Contract No. DE-AC36-08GO28308).

References

[1] Feldman DJ, Margolis RM. Q4 2018/q1 2019 solar industry update, Tech. rep., National Renewable Energy Lab. (NREL), Golden, CO (United States); 2019.
[2] Akhter MN, Mekhilef S, Mokhlis H, Shah NM. Review on forecasting of photovoltaic power generation based on machine learning and metaheuristic techniques. IET Renew Power Gener 2019;13(7):1009–23.
[3] Feng C, Cui M, Hodge B-M, Lu S, Hamann H, Zhang J. Unsupervised clustering-based short-term solar forecasting. IEEE Trans Sustain Energy 2018;10(4):2174–85.
[4] Yang D. On post-processing day-ahead nwp forecasts using kalman filtering. Sol Energy 2019;182:179–81.
[5] Jang HS, Bae KY, Park H-S, Sung DK. Solar power prediction based on satellite images and support vector machine. IEEE Trans Sustain Energy 2016;7(3):1255–63.
[6] Feng C, Cui M, Hodge B-M, Zhang J. A data-driven multi-model methodology with deep feature selection for short-term wind forecasting. Appl Energy 2017;190:1245–57.
[7] Huang R, Huang T, Gadh R, Li N. Solar generation prediction using the arma model in a laboratory-level micro-grid. In: 2012 IEEE third international conference on smart grid communications (SmartGridComm), IEEE; 2012. p. 528–33.
[8] Wan C, Zhao J, Song Y, Xu Z, Lin J, Hu Z. Photovoltaic and solar power forecasting for smart grid energy management. CSEE J Power Energy Syst 2015;1(4):38–46.
[9] Mandal P, Madhira STS, Meng J, Pineda RL, et al. Forecasting power output of solar photovoltaic system using wavelet transform and artificial intelligence techniques. Proc Comput Sci 2012;12:332–7.
[10] Sun M, Feng C, Chartan EK, Hodge B-M, Zhang J. A two-step short-term probabilistic wind forecasting methodology based on predictive distribution optimization. Appl Energy 2019;238:1497–505.

[11] Munkhammar J, Widén J, Hinkelman LM. A copula method for simulating correlated instantaneous solar irradiance in spatial networks. Sol Energy 2017;143:10–21.
[12] Smith CJ, Bright JM, Crook R. Cloud cover effect of clear-sky index distributions and differences between human and automatic cloud observations. Sol Energy 2017;144:10–21.
[13] Van der Meer DW, Widén J, Munkhammar J. Review on probabilistic forecasting of photovoltaic power production and electricity consumption. Renew Sustain Energy Rev 2018;81:1484–512.
[14] Lauret P, David M, Pedro HT. Probabilistic solar forecasting using quantile regression models. Energies 2017;10(10): 1591.
[15] Verbois H, Rusydi A, Thiery A. Probabilistic forecasting of day-ahead solar irradiance using quantile gradient boosting. Sol Energy 2018;173:313–27.
[16] Yang Y, Li S, Li W, Qu M. Power load probability density forecasting using gaussian process quantile regression. Appl Energy 2018;213:499–509.
[17] Sheng H, Xiao J, Cheng Y, Ni Q, Wang S. Short-term solar power forecasting based on weighted gaussian process regression. IEEE Trans Industr Electron 2017;65(1):300–8.
[18] Kim CK, Kim H-G, Kang Y-H, Yun C-Y, Kim SY. Probabilistic prediction of direct normal irradiance derived from global horizontal irradiance over the Korean Peninsula by using monte-carlo simulation. Sol Energy 2019;180:63–74.
[19] Massidda L, Marrocu M. Quantile regression post-processing of weather forecast for short-term solar power probabilistic forecasting. Energies 2018;11(7):1763.
[20] Huang J, Perry M. A semi-empirical approach using gradient boosting and k-nearest neighbors regression for gefcom2014 probabilistic solar power forecasting. Int J Forecast 2016;32(3):1081–6.
[21] Alessandrini S, Delle Monache L, Sperati S, Cervone G. An analog ensemble for short-term probabilistic solar power forecast. Appl Energy 2015;157:95–110.
[22] Zhang J, Draxl C, Hopson T, Delle Monache L, Vanvyve E, Hodge B-M. Comparison of numerical weather prediction based deterministic and probabilistic wind resource assessment methods. Appl Energy 2015;156:528–41.
[23] Wang Y, Zhang N, Tan Y, Hong T, Kirschen DS, Kang C. Combining probabilistic load forecasts. IEEE Trans Smart Grid 2018;10(4):3664–74.
[24] Xie J, Hong T. Temperature scenario generation for probabilistic load forecasting. IEEE Trans Smart Grid 2016;9(3):1680–7.
[25] Liu B, Nowotarski J, Hong T, Weron R. Probabilistic load forecasting via quantile regression averaging on sister forecasts. IEEE Trans Smart Grid 2015;8(2):730–7.
[26] Breinl K, Turkington T, Stowasser M. Simulating daily precipitation and temperature: a weather generation framework for assessing hydrometeorological hazards. Meteorol Appl 2015;22(3):334–47.
[27] Hontoria L, Rus-Casas C, Aguilar JD, Hernandez JC. An improved method for obtaining solar irradiation data at temporal high-resolution. Sustainability 2019;11(19):5233.
[28] Sun M, Feng C, Zhang J. Conditional aggregated probabilistic wind power forecasting based on spatio-temporal correlation. Appl Energy 2019;256:113842.
[29] Panamtash H, Zhou Q, Hong T, Qu Z, Davis KO. A copula-based bayesian method for probabilistic solar power forecasting. Sol Energy 2020;196:336–45.
[30] Louie H. Characterizing and modeling aggregate wind plant power output in large systems. In: Power and energy society general meeting, 2010 IEEE, IEEE; 2010. p. 1–8.
[31] Wang Z, Wang W, Liu C, Wang Z, Hou Y. Probabilistic forecast for multiple wind farms based on regular vine copulas. IEEE Trans Power Syst 2018;33(1):578–89.
[32] Cui M, Krishnan V, Hodge B-M, Zhang J. A copula-based conditional probabilistic forecast model for wind power ramps. IEEE Trans Smart Grid 2018;10(4):3870–82.
[33] Hartley HO. Maximum likelihood estimation from incomplete data. Biometrics 1958;14(2):174–94.
[34] Tang C, Wang Y, Xu J, Sun Y, Zhang B. Efficient scenario generation of multiple renewable power plants considering spatial and temporal correlations. Appl Energy 2018;221:348–57.
[35] Rüschendorf L. On the distributional transform, sklar's theorem, and the empirical copula process. J Stat Plan Inference 2009;139(11):3921–7.
[36] Yan J, et al. Enjoy the joy of copulas: with a package copula. J Stat Softw 2007;21(4):1–21.
[37] Birchfield AB, Xu T, Gegner KM, Shetye KS, Overbye TJ. Grid structural characteristics as validation criteria for synthetic networks. IEEE Trans Power Syst 2016;32(4):3258–65.
[38] Sengupta M, Xie Y, Lopez A, Habte A, Maclaurin G, Shelby J. The national solar radiation data base (nsrdb). Renew Sustain Energy Rev 2018;89:51–60.
[39] Freeman J, DiOrio N, Blair N, Guittet D, Gilman P, Janzou S. Improvement and validation of the system advisor model. Tech rep, National Renewable Energy Laboratory; 2019.
[40] Cui M, Zhang J, Hodge B-M, Lu S, Hamann HF. A methodology for quantifying reliability benefits from improved solar power forecasting in multi-timescale power system operations. IEEE Trans Smart Grid 2017;9(6):6897–908.